Experimental Validation of Periodic Codes for PON Monitoring

Mohammad M. Rad, Habib Fathallah, Sophie LaRochelle, and Leslie A. Rusch
ECE Dept. Université Laval, Québec, Québec, Canada G1K 7P4
Email:rusch@gel.ulaval.ca

***Abstract*— In this paper we investigate both experimentally and via simulation the monitoring of fiber link quality in a PON using optical coding technology. We use a new, simple and cost-effective coding scheme well adapted to the monitoring application, namely *periodic* coding. We discuss design issues for periodic coding and the optimal detection criteria. We develop a reduced complexity maximum-likelihood sequence estimation (RC-MLSE) algorithm for monitoring. We conduct experiments to validate our detection algorithm using four periodic encoders that we designed and fabricated. These encoders were placed at roughly equal distances (within a meter) to represent a partial return from a very high density (geographically) PON. The measured data were fed into our detection algorithm and the exact location of each subscriber was correctly identified. Using the experimental data for the encoder's impulse responses, we completed Monte-Carlo simulations for more realistic PON geographical distributions with randomly located customers. Error-free detection is achieved. We also highlight the importance of averaging to remedy the power/loss budget limitations in our monitoring system to support higher network sizes.**

***Index Terms*—Detection probability (P_D), maximum-likelihood sequence detection (MLSE), network monitoring, Periodic coding, PON, optical time domain reflectometry (OTDR).**

I. Introduction

MONITORING of a passive optical network (PON) can significantly reduce the operational expense (OPEX) for both operators and customers, and so plays an important role in the deployment of future access networks [1-4]. The growth PONs (to support more customers per fiber with higher data rates and better quality of service) increases both the importance and the complexity of network monitoring.

Optical-time-domain reflectometry (OTDR) is efficient for testing optical devices and monitoring of point-to-point (PTP) networks [1]. OTDR is used for the installation and maintenance of tree architecture PONs, by testing each distribution drop fiber (DDF) segment separately from the remote node to the customer premise and vice-versa. However, OTDR is less suitable for centralized (i.e., from the central office) monitoring of point-to-multipoint (PMP) networks like fiber-to-the-home (FTTH) PONs [1,4]. The backscattering signal of each branch in a PMP network is partially masked by that of the other branches. A few solutions have been proposed to adapt the standard OTDR to a PON, among which the most well-known is the technique based on reference reflectors [1,4]. A reference reflector at each branch end provides information on the integrity of that branch. This method is unable to localize a non-reflective fiber break or loss. The technique is not viable when branches are located very closely or at the same distance, thus drops are required to have distinct lengths. While feasible at system installation, this approach is unmanageable during incremental expansion and routine maintenance. As the network size increases, the reliability and manageability of this technique decreases.

In [5], we introduced a modified optical code division multiplexing (OCDM) scheme for centralized monitoring of PONs that is architecture agnostic. The reference reflector is replaced by a coding mirror. The multiple reflections from subscribers are distinguishable by proper decoding, and customers no longer need to be connected to the central office (CO) with unequal fiber length. The geographical distribution of the customers has significant impact on the performance and we developed a Monte Carlo simulation that statistically averaged over subscriber locations [6].

We analyzed optical orthogonal codes (first proposed for coded data) for the monitoring application, examining both one-dimensional and two-dimensional codes [6,7]. In [8] we developed codes better adapted to location detection (instead of using codes developed for data detection), whose implantation costs were also significantly reduced from those studied in [5,6,7]. These new, simple and cost-effective codes were periodic in nature. While [8] examined these codes to explore their performance in terms of auto and cross correlation, in this paper we examine optimal detection algorithms that far outperform correlation for periodic codes (PC).

II. PON Monitoring Using Optical Coding

A. Principle of Operation

As illustrated in Fig.1, a U-band (i.e., 1625-1675 nm devoted for PON monitoring [1,2]) short pulse with peak power P_s and duration T_s is transmitted through the feeder, split into N sub-pulses at the remote node (RN), each of which is encoded and reflected back to the CO by a dual function device: coder and mirror we refer as coding mirrors (CM_i, i =1 to N) [5]. Note that the monitoring signals are carried on λ_m while the data wavelength is λ_d in Fig.1. Each DDF is terminated by a CM with a unique code, and is located physically close to the optical network terminal (ONT). The CO monitoring equipment receives the accumulation of all sequences coming from CMs. Information on an individual DDF is discernable at the CO by exploiting code structure.

Features of the encoded sequences could be used to assess

978-1-4244-4148-8/09/$25.00 ©2009

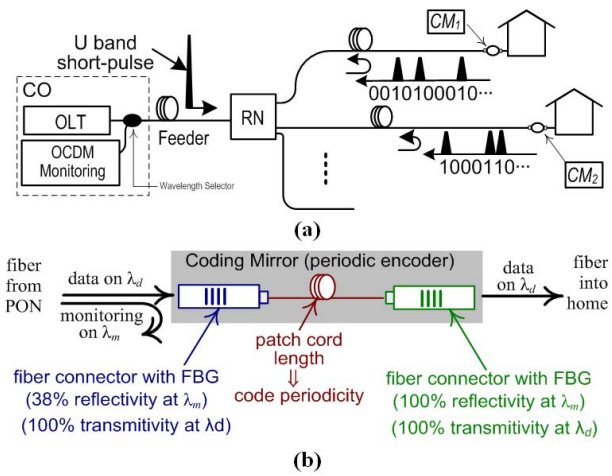

Figure 2 a) Optical coding based PON monitoring, b) the structure of periodic encoder

the link quality for individual fiber branches. For instance, for a break in a DDF, no corresponding autocorrelation peak is observed; similarly, the lack of auto-correlation peaks for all CMs identifies a fault in the feeder [5]. Decreasing autocorrelation indicates the link between the central office and ONT is degrading. When all auto-correlation peaks decrease, the problem originates in the feeder segment. In practical PON installations, network segments consist of bundles of fibers with different counts. When an external event occurs (*i.e.,* breaks or bends), all channels in that cable are affected.

B. Periodic Coding (PC)

Periodic codes can be implemented using only two fiber Bragg gratings written for the same waveband; the first is partially reflective, while the second acts as a frequency selective mirror. By inserting a patch cord between the gratings, an optical cavity is formed [8], see Fig. 1b. A single incident pulse generates an infinite length, periodic sequence of multilevel sub-pulses from the cavity. A code is determined by the number of silent pulse intervals separating the multilevel pulses, or equivalently the period of the code, p_i. The length l_i patch cord determines the period p_i which in turn distinguishes different users. For a pulse width of T_s, the periodicity p_i and l_i are related by

$$l_i = cp_iT_S/2n_g \qquad (1)$$

where c and n_g are the speed of light and the fundamental mode group index that determines the time of flight. The grating pair is the same for all CMs and only their separation l_i (equivalently the period number p_i) changes with the code. As explained in [8], the second grating of the encoder, tuned to reflect the monitoring wavelength, eliminates the requirement for a separate wavelength selector per subscriber to demultiplex the data band [5]. Periodic CMs are small in size and easy to handle.

III. Periodic Encoder Design

This section focuses on the design of the gratings required to make periodic encoders. Further details can be found in [8].

A. Monitoring Wavelength

The most common wavelengths for out-of-band monitoring are 1625 nm or 1650 nm [9,10,11]. At 1650 nm we have higher sensitivity to macro-bends than at 1625 nm, and more strict isolation is required at 1625nm as it is closer to the data band (L Band, *i.e.*, 1565-1625nm). For these reasons, the ITU-T recommends 1650 nm [1]. Although 1625 nm has not yet been adopted in the standard, it is more economical and readily available, while 1650 nm lasers are still very expensive. We use a 1650 nm monitoring wavelength [9]; the same design could be applied at 1625nm. In our experimental verification, we operate at 1550 nm due to equipment availability.

B. Reflectivity

As explained in [8], to concentrate the total energy in a few reflected pulses (for shorter codes) the grating reflectivities are found to be R_1=38% and R_2=100% for all encoders. This fixes the transmission loss of the gratings, *i.e.*, T_1=2.1dB and T_2=∞ respectively in the wavelength interval around the monitoring wavelength. Typical values of T_2=50dB can be achieved via conventional FBG fabrication [9,11]. Again recall that all the encoders have the same specifications for FBG1 and FBG2. The implemented spectral characteristics of the FBGs are given in Fig.2.

C. Bandwidth

In choosing the bandwidth, d, of our encoder gratings we must take into account two factors: 1) the effect of this choice on the isolation of data and monitoring bands and 2) the availability of bandwidth and spectral efficiency trade-offs. We can choose a rejection bandwidth d that is spectrally efficient, so long as it also returns a large portion of the energy from the source and is tolerant to some source drift. While the U band is 50 nm wide, we may wish to create several bands, either for monitoring or for other information bands. In our experimentation we fix d = 12 nm as a reasonable compromise [11].

D. Fiber Length Optimization

Once the pulse duration, T_s, of the monitoring signal is

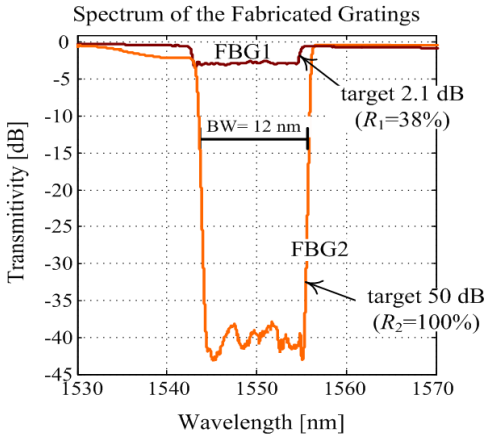

Figure 1 Experimental implementation of FBG1 and FBG2 forming the periodic encoder.

978-1-4244-4148-8/09/$25.00 ©2009

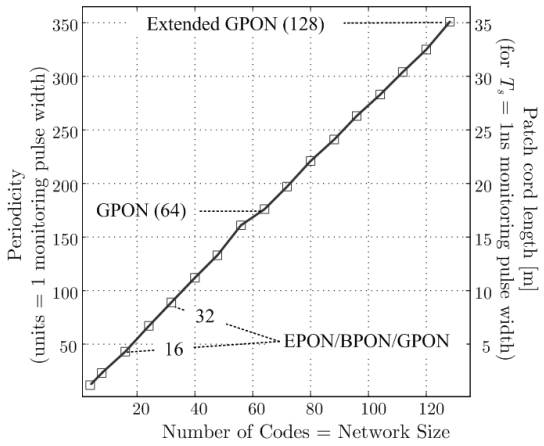

Figure 3 Code periodicity (patchcord length) versus the network size for periodic code.

fixed, the length of the fiber joining FBG1 and FBG2 is determined per (1). The pulse width thus impacts the compactness of our encoders. It also impacts the sampling rate required at the digital receiver. For our simulations and experiments we have fixed T_s = 1 ns, although other system designers may seek another compromise.

For results reported in this paper, we generate codes using the simple algorithm developed in [8], fixing the code weight (to w=4) and minimizing the maximum of cross correlation (to 1). Having the periodicity of each code p_i (i=1,…,N) by this method, we have the corresponding fiber length l_i per (1). The simple structure of the periodic codes enables us to produce any desired number of codes. In Fig.4, we plot the periodicity (maximum required patch cord length) versus the network capacity for a T_s = 1 ns pulse width. Periodic coding provides a practical solution for current standards of PONs as well as future expansion [1,2]. For instance, for a GPON with 32 branches, the first periodic code CM requires l_1=0.6m patch cord, while the last one requires l_{32}=8.3m patch cord. New CMs (for new subscribers) are simple to design and fabricate, hence our solution is flexible and scalable.

IV. Transmitter and Receiver Considerations

A. Transmitter Module

The transmitter module has a U band laser that launches a short pulse of duration T_s into the network. For our analysis we assume a 1650 nm monitoring wavelength [9]-[11], and a light source side band suppression ratio below -80dB for good data isolation [11]. The repetition rate T_r for pulse transmission is constrained by the distance between the CO and the farthest ONT. Repetition rates on the order of kilohertz would be typical. Both direct and indirect modulation schemes can be used to generate the U band monitoring pulses. Experimentally, we consider an externally modulated spectrum sliced broadband light source (SS-BBS) operating at 1543 nm. Note that BBS has been previously used for the monitoring applications [12]. Direct modulation would incur lower losses and reduce cost.

B. Receiver Module

All decoding functions are implemented in the electronics following simple photodetection, as seen in Fig.3. No programmable optical decoding is required, significantly reducing the cost (and the size) of the receiver equipment as compared to other optical coding solutions. In previous proposals, the CO needs programmable optical decoders or a bank of all-optical decoders to decode the signal of each decoder [5]-[7]. By implementing the decoding in electronics, we no longer need this expensive, complex, and bulky all-optical module. In addition**,** electronic processing also reduces power insertion and decoding loss [8]. The sampling rate is determined by the pulse width. For our choice of T_s = 1 ns, gigahertz sampling is required and readily available in affordable electronics. The ADC should provide good quantization for our detection algorithm, such as 8 or 10 bits per sample; such ADCs are a mature, commercially available technology.

Digital signal processing will accomplish multiple functions. First among them is the averaging of received waveforms for noise reduction [13]. As no training sequence is used, the processing must perform pulse synchronization. These functions are not addressed in this article, as we focus on fiber fault detection beginning in the next section.

V. Decoding Algorithm for Error Free Detection

Detection requires information on encoder impulse responses, network loss budget, and characteristics of the transmitted pulse. We assume this information is known. Our detection algorithm has three objectives

1. *Fault detection*: identify the presence or not of all subscribers without prior knowledge of subscriber location (i.e., fiber length between the remote note and the subscriber location)
2. *Self-discovery:* estimate the fiber length of each subscriber
3. *Channel condition monitoring*: estimate signal features for each subscriber

Note that the primary mission (objective one) is to identify unhealthy subscriber lines; a binary decision is made for each subscriber. The secondary mission is to gain information on the quality of each subscriber line. For this, the estimation of the subscriber position (or equivalently the fiber length) is essential so that signal processing can be directed at this portion of the returned signal. At a minimum, objective two will provide information on signal strength. Additional signal processing can be used to determine additional features and accomplish the third objective, although this is not explored in this article.

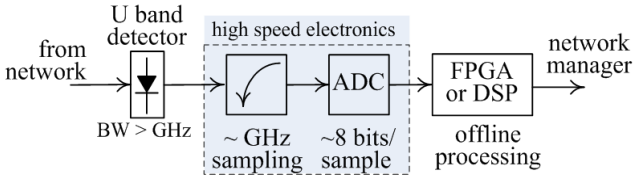

Figure 4 Receiver architecture

978-1-4244-4148-8/09/$25.00 ©2009

A. Standard Maximum-Likelihood Sequence Detection

Optimal detection of a single subscriber coded signal in additive white Gaussian noise requires a simple matched filter or correlator. Due to the simultaneous presence of multiple subscriber signals, the optimal detection algorithm must consider all possible states of the network before deciding if each particular subscriber signal is present [14]. The received signal must be compared in turn with an expected return signal for each possible network configuration; this constitutes a classic maximum likelihood sequence estimation (MLSE) algorithm. A network configuration refers to the presence or not of a subscriber signal, as well as the lengths of fiber between the remote node and each subscriber.

The search space of the MLSE algorithm depends on 1) network size (number of subscribers), 2) coverage area (maximum fiber length from remote node to subscriber), and 3) sampling rate of the monitoring system (samples per pulse duration). Even moderate values of network parameters yield in exceedingly large search space. For example, a PON with only $N = 4$ subscribers, with a maximum fiber run of $l_{max} = 12.6$ m (coverage area of 500 m^2) and a receiver sampling rate of $R_s = 1$ Gs/s requires 126^4 comparisons for MLSE.

A brute force algorithm for MLSE is prohibitively complex, especially as network size grows. The most commonly employed algorithm for MLSE is the Viterbi algorithm that associates a finite state machine with the sequences to estimate. The Viterbi algorithm exploits the state transitions to eliminate at each symbol interval sequences with low probability that need not be retained for consideration. The Viterbi algorithm is not only less computationally complex, it is also very efficient in terms of memory usage. The continuous transmission of symbols whose values are influenced by preceding symbols (as with intersymbol interference and forward error correction) can be described by a finite state machine and is therefore compatible with the Viterbi algorithm. Unfortunately no finite state machine can be easily associated with the PON monitoring system, so the Viterbi solution is not applicable.

Note that the reduced memory requirements for the Viterbi algorithm are due to the processing of sequences at each symbol interval and retention of only potentially "winning" sequences. This is an extremely powerful and important aspect of the Viterbi algorithm for data communications. The PON monitoring problem is very different. For monitoring we need to use signal averaging to improve the signal to noise ratio, as is common in OTDR methods [13]. For this reason, memory is reserved for the sampled return signal; moderate delay for averaging and processing (milliseconds to seconds) is acceptable for this application. Therefore the MLSE algorithm can process the entire sampled signal return without an overhead for memory. We next present an algorithm for MLSE computation that is adapted to the PON monitoring problem and to periodic codes in particular [14].

B. Reducing MLSE Complexity for PON Monitoring

There are two characteristics of the PON monitoring return signal that we will exploit to accelerate the MLSE. As in the Viterbi algorithm, we seek to eliminate low probability network configurations, so that only highly probable configurations need be compared in the MLSE search. The first characteristic we will exploit is the *correlation distance* of a particular code in the network, and the second is the structure of the periodic codes.

The *correlation distance* of a code is defined by

$$l_{CD}^{(n)} = \frac{p_n T_s (w-1)c}{n_g} \quad n = 1,\ldots,N$$

where p_n is the periodicity of the corresponding code and w-1 is the number of periods between the first and last pulse [6]. Only subscribers whose fiber lengths differ from that of user n by less than $l_{CD}^{(n)}$ may potentially interfere with user n. The geographical distribution of the ONTs will impact the number of subscribers falling within this *correlation distance*.

Due to the correlation distance, in PON monitoring we expect only a relatively small subset of subscribers will contribute to multiple access interference (MAI), in contrast with data communications, where all active subscribers contribute to MAI. In our algorithm we will process signals in the order of increasing MAI. Signal returns without interference will be identified first and eliminated from the subsequent searches. Signals with one interferer will be identified next, etc.

The periodic structure of the codes allows for a simple test for the presence of a code. Once a single pulse has been identified, we search in time to see if another w-1 pulses are present at time intervals corresponding to the code period under test. We will use a digital sliding correlator to identify possible locations for specific subscriber returns.

C. RC-MLSE Algorithm

The algorithm can be divided in two parts as illustrated in Fig.5. The first part uses N parallel sliding (matched-filter) correlators of the periodic codes to generate our sufficient statistic. Interference-free subscribers are detected and localized without requiring an MLSE search. This step also determines the uncertainty space for MLSE searches of the remaining subscriber status and location. The second part performs a serial search on possible status/locations; at each iteration, progressively more computationally complex searches are made.

We make the following assumptions. We have N codes with periodicities $\{p_n\}_{n=1}^{N}$ corresponding to N subscribers; $|p_n|$ is the length of the n^{th} code; the N^{th} code is the longest code; and a vector of length N_s is formed from the sampled return.

i) Identifying Interference-Free Users

1. Run N simple (digital) sliding matched-filter correlators against the sampled return signal. Each sliding correlator outputs a vector $\underline{\mathbf{C}}_n$ with a one as an element if it is possible that code p_n begins at that time sample. Note that at each sample, the correlator needs only identify a minimum height at the non-zero positions of code p_n proceeding from that specific time sample.
2. The vectors $\underline{\mathbf{C}}_n$ with hamming weight one (with only one

978-1-4244-4148-8/09/$25.00 ©2009

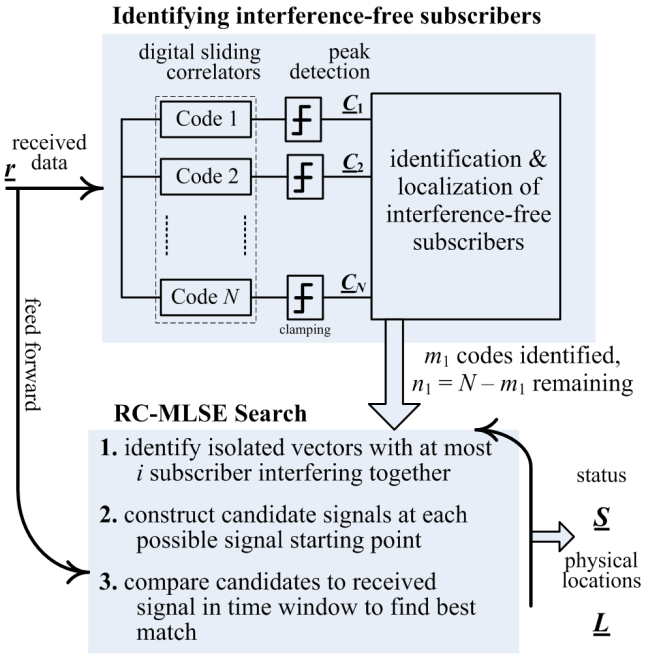

Figure 5 Reduced Complexity MLSE algorithm

non-zero element) are identified and

- the fiber length to subscriber n is deduced from the position of the non-zero entry in vector $\underline{\mathbf{C}}_n$; the n^{th} link is declared healthy and its location is noted;
- the n^{th} code is removed from the set of codes to be searched, so it is not considered in future iterations;
- for vectors $\underline{\mathbf{C}}_n$ with hamming weight zero the n^{th} subscriber line is declared faulty.

3. The vectors $\underline{\mathbf{C}}_n$ are examined to see if there is

- any window of length $2|p_n|$ where only $\underline{\mathbf{C}}_n$ (an no other $\underline{\mathbf{C}}_i$) has a single non-zero element, *i.e.*, an isolated peak.
- the n^{th} fiber length is deduced from this window; it is declared healthy and its location is noted;
- the n^{th} code is removed from the set of codes to be searched;

ii) Iterative RC-MLSE search

1. At iteration i, the collection of unresolved $\{\underline{\mathbf{C}}_n\}$ are examined to find windows of length $2|p_n|$ where only i vectors have non-zero elements; a collection of i mutually interfering users is thus identified. For this collection,

- we examine if they are isolated; a collection of i vectors is isolated if and only if they only interfere together;
- if the collection is not isolated, i is increased and the algorithm searches for larger collections of isolated mutually interfering vectors.

2. For the identified vectors (subscribers), we generate candidate signals that sum the i codes with starting times found in the $\{\underline{\mathbf{C}}_n\}$ for the window; if a correlator vector has more than one non-zero element in the window, a candidate is generated based on the each possible code starting point (non-zero element).

3. Once all possible candidate signals have been calculated, they are compared to the received signal $\underline{\boldsymbol{r}}$. The best match is retained as an estimate.

The algorithm continues looking for increasingly larger numbers of mutually interfering users. Once such windows are no longer identifiable, an exhaustive search is made of the remaining unidentified $\{\underline{\mathbf{C}}_n\}$.

D. Challenges of RC-MLSE Algorithm

Clearly the RC-MLSE offers significant computational savings by exploiting the PON monitoring environment and periodic code structure. Analysis is problematic as the complexity is a function of the geographic distribution of subscribers. In the balance of this paper, we validate our algorithm experimentally, testing a severe case where up to four subscribers are virtually collocated – the difference is fiber lengths is minimal. As we will see, the RC-MLSE algorithm detects and localizes all four encoders, enabling live, in-service PON monitoring.

The clamping threshold (in the first stage of the algorithm) can be fixed under normal healthy conditions. When new subscribers are added, the uncertainty in the threshold increases. The receiver can determine numerically (via iteration) the threshold by gauging performance on already known subscribers. Similarly, an iterative approach would be necessary to set the threshold on a new network installation. Thus we anticipate that computation requirements would be greater at network setup as opposed to steady state. The increase however would be linear in the number of thresholds tested.

VI. Experimental Setup

As explained in section III, we fabricated four periodic encoders; the FBG characteristics are given in Fig. 2b. We implemented a 12 nm rejection bandwidth, with center wavelength of 1550 nm. We used code weight of $w = 4$ and cross correlation of one, to produce codes with periodicity of $p_1 = 6$ (60 cm), $p_2 = 7$ (70 cm), $p_3 = 13$ (130 cm), and $p_4 = 16$ (160 cm). We excluded the code with periodicity of one due to difficulty in fabrication.

A. Experimental Setup

The experimental setup is illustrated in Fig.6. The setup has two main sections: the central office, and a network of four subscribers with distinct CMs. For experimental convenience, the monitoring source is a broadband light source (BBS) with optical bandwidth of 40 nm. The BBS is filtered (spectrally sliced) by a narrowband tunable filter with a 0.2 nm optical passband. The filtered BBS is pre-amplified by an erbium doped fiber amplifier (EDFA). A Mach-Zehnder (MZ) external modulator is used to generate the monitoring pulse with duration of T_s =1 ns (1GHz). The MZ is driven with a repetition interval of 500 μs[1]. To compensate the loss of the MZ we post amplified the modulated signal. Optical filters are used after EDFAs to suppress the amplified spontaneous emission (ASE) noise.

[1] This corresponds to maximum distance of 50 km between the CO and CMs.

978-1-4244-4148-8/09/$25.00 ©2009
This full text paper was peer reviewed at the direction of IEEE Communications Society subject matter experts for publication in the IEEE "GLOBECOM" 2009 proceedings.

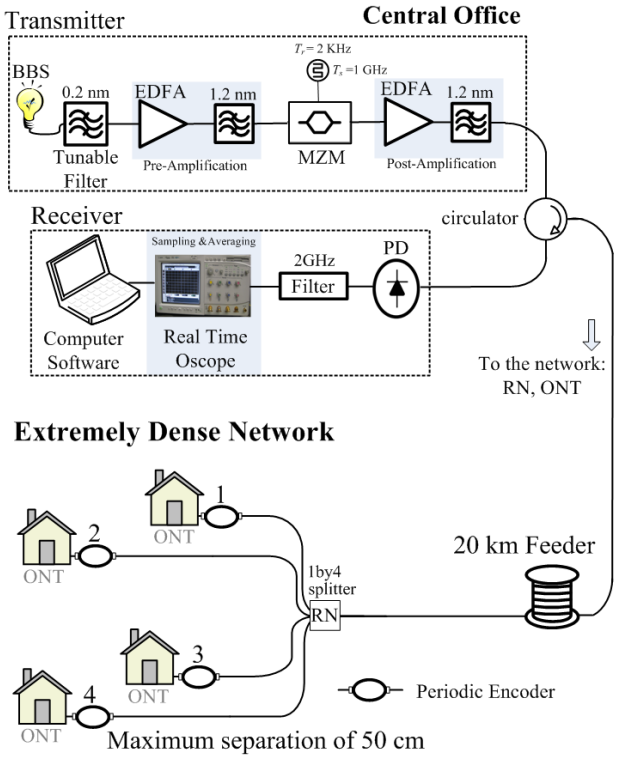

Figure 7 Experimental setup for the monitoring of a high density 4 customer PON

Using the setup in Fig.6, in Fig.7 we plot the time domain response of the encoders to the 1 ns probe pulse. The center wavelength of the monitoring source was tuned for the best possible impulse response and in our case it was 1543.3 nm. As is illustrated, the multilevel codes are nearly identical except for differences in code period. The DC value of each code does vary slightly due to variations in the grating spectra and contributions from the filtered ASE. In particular, the impulse response of the encoders is very sensitive to the reflectivity of the first grating.

The maximum transmitted power was kept low enough not to induce any non-linearity. The monitoring pulse is sent to the network using a circulator; a 20 km roll of fiber plays the role of feeder, and a 1×4 coupler serves as the RN. The fibers to each home are of roughly equal lengths (within 45 cm as seen in Fig.7) corresponding to a very dense PON. Note that due to the round-trip of the monitoring pulse through the network, the total loss is 2×20 km×0.2 dB/km (feeder) + 2×6 dB (splitter) = 20 dB. A real-time oscilloscope sampling at 10 Gs/s was used to capture the measured trace. The oscilloscope provides both sampling and averaging.

Recall that filtering a BBS increases the relative intensity noise (RIN) [13]. As a result, our monitoring light source significantly suffers from RIN. However, in our application using averaging we can effectively remove the RIN of the source; reducing the RIN power by ~24 dB for 256 averaging. Similar reductions are experienced in beat noise, shot noise, and thermal noises. Our measurement is therefore interference limited.

Figure 7e shows the total received signal when all four encoders are connected to the network. Recall that for a 17 ps/km/nm dispersion factor, the total amount of dispersion is 136ps (0.2 nm optical bandwidth) which is negligible compared to the transmitted pulse width.

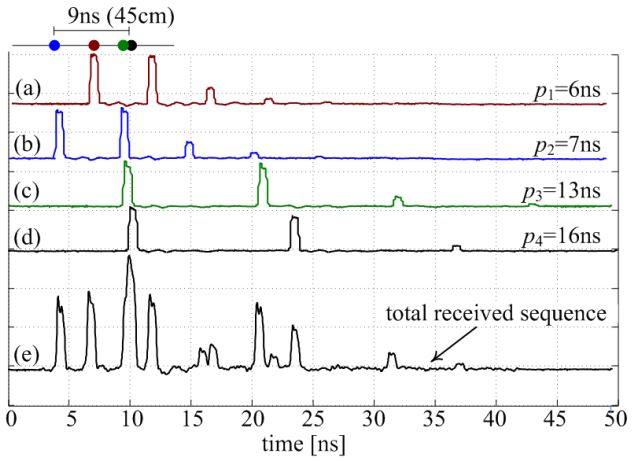

Figure 6 Experimental traces of isolated subscribers (a)-(d), and when all four subscribers are present (e); signals averaged over 256 traces to reduce noise

B. Simulation Results

The data captured in Fig. 7e was sent to our RC-MLSE algorithm. While having encoders (equivalently subscribers) less than a meter apart is not realistic, this represents a worst case scenario in that the probability of interference is high. In a larger network, close proximity may occur for a subset of subscribers, hence we tested experimentally this extreme case in our detection algorithm. Our RC-MLSE algorithm correctly determined the fiber length to all CMs to within a pulse width (1 ns or ±10 cm).

These experimental results were also used as realistic traces of individual returns (i.e., taking encoders returns one-by-one). These returns were used in our simulator of larger, more realistic networks. Using the measured traces for the encoders' impulse responses from our experimental setup, we completed Monte-Carlo simulation (10^5 realizations) over a 10^4 m^2 coverage area. The subscriber locations followed a uniform radial (UR) distribution [6]. In all cases, we were able to detect and localize correctly all encoders; error-free detection was achieved (P_D=1).

VII. Loss Budget Limits: The Importance of Averaging

As mentioned earlier, due to the round-trip path of the monitoring pulses, the insertion loss of passive elements is doubled, imposing strict limitations on the total loss budget of our monitoring system. In particular, higher number of customers leads to higher splitting ratios at the RN and so more critical power/loss budget. For instance, for a 16 (32) customer PON, the total insertion loss only due to RN splitting is 24 (30) dB.

Note that increasing the transmitted power to mitigate the loss budget increases nonlinear effects, and cannot be employed without restraint. To avoid nonlinear impairments the launched power should be kept smaller than approximately

978-1-4244-4148-8/09/$25.00 ©2009
This full text paper was peer reviewed at the direction of IEEE Communications Society subject matter experts for publication in the IEEE "GLOBECOM" 2009 proceedings.

10 dBm for a single mode fiber. Our strategy for higher loss budget costs relies on signal averaging. By averaging, i.e., repeating the measurement many times, we reduce noise and increase our signal-to-noise-ratio (SNR) [13]. The dynamic range and sensitivity of the monitoring receiver significantly increases. As we are monitoring and not transmitting data, the temporal overhead for averaging is not burdensome.

When employing signal averaging, the measurement becomes interference-limited; quantum limited detection is achieved. Consequently the minimum detectable power is limited only by the detector's dark current. Therefore, the monitoring receiver is able to detect very small powers comparable to dark current. As an example, consider a CO that uses a PIN detector with 1 nA dark current and unitary responsivity [13], a total 10 dBm launched power for the monitoring signal, and a modulator with infinite extinction ratio. In this case, the DC current in the absence of monitoring pulses is 1 nA, minimum detectable power of 1nW. Now consider 10 dB margin for the received monitoring pulse power compared to the dark current DC level; *i.e*., set the minimum acceptable power for monitoring pulse to 10 nW. The total permissible (round-trip) loss is 60 dB. Thus we are able to support high network sizes such as 32 (30 dB loss at the RN) with long fiber lengths such as 20 km (12 dB loss). Recall that the loss/budget can be further improved by using high gain avalanche photo-diodes (APDs) with very low dark currents [13].

VIII. Conclusion

In this paper, we experimentally investigated optical coding based PON monitoring. We address the design issues of recently proposed periodic encoders, fabricated them and used them for fiber link quality monitoring of a PON. Four customers at extreme proximity, simulating a high density PON, were examined in our experiments. We developed a reduced complexity maximum likelihood sequence detection (RC-MLSE) algorithm which optimally distinguishes, detects, and localizes each encoder in the network. The measured data were fed into our algorithm. Our simulation results validate our algorithm in detecting and localizing all encoders. The importance of averaging is also highlighted to remedy the loss/budget limitations.

References

[1] A. Girard, "FTTx PON technology and testing," *EXFO Electro-Optical Engineering Inc*., Canada, 2005, ISBN 1-55342-006-3.

[2] http://www.ftthcouncil.org/

[3] R. Davey, and D. Payne, "The future of optical transmission in access and metro networks-An operator's point of view," *European Conf. on Optical Commun.* (ECOC), We 2.1.3, 2005.

[4] F. Caviglia, and V. C. Biase, "Optical maintenance in PONs," *European Conf. on Optical Commun.* (ECOC), Madrid, Spain, pp. 621-625, 1998.

[5] H. Fathallah, and L. A. Rusch, "Code division multiplexing for in-service out-of-band monitoring," *J. Optical Networking*, vol. 6, no. 7, pp. 819-829, July 2007.

[6] M. M. Rad, H. Fathallah, and L. A. Rusch, "Effect of PON geographical distribution on monitoring by optical coding," in *Proc. European Conf. on Optical Commun.* (ECOC), paper 7.6.6, Berlin, Germany, 2007.

[7] M. M. Rad, H. Fathallah, and L. A. Rusch, "Fiber fault monitoring for passive optical networks using hybrid 1D/2D coding scheme," *IEEE Photonic Technology Letter*, Vol. 20, No. 24, pp. 2054-2056, Dec. 2008.

[8] H. Fathallah, M. M. Rad, L. A. Rusch, "PON Monitoring: Periodic Encoders with Low Capital and Operational Cost," *IEEE Photonic Technology Letter*, Vol. 20, No. 24, pp. 2039-2041, Dec. 2008.

[9] N. Gagnon, A. Girard, M. Leblanc, "Considerations and recommendations for in-service out-of-band testing on live FTTH networks," *IEEE Optical Fiber Commun. Conf.* (OFC*)*, paper NWA3, March 2006.

[10] N. Nakao, H. Izumita, T. Inoue, Y. Enomoto, N. Araki, and N. Tomita, "Maintenance method using 1650 nm wavelength band for optical fiber cable networks," *IEEE J. Lightwave Technology*, Vol. 19, No. 10, pp. 1513-1520, Oct. 2001.

[11] N. Honda, H. Izumita, and M. Nakamura, "Spectral filtering criteria for U-band test light for in-service line monitoring in optical fiber networks," *IEEE J. Lightwave Technology*, Vol. 24, No. 6, pp. 2328-2335, June 2006.

[12] S. B. Park, D. K. Jung, H. S. Shin, D. J. Shin, S. Hwang, Y. Oh, and C. Shim, "Optical fault monitoring method using broadband light source in WDM-PON," *Electronic Letter*, vol. 42, no. 4, Feb. 2006.

[13] D. Deickson, "Fiber optic test and measurements," *Prentice Hall*, 1997, ISBN-10: 0135343305.

[14] S. Benedetto, E. Biglieri, "Principles of digital transmission: with wireless application," *Springer*, 1999, ISBN-0306457539.

978-1-4244-4148-8/09/$25.00 ©2009